

Atomistic Boron-Doped Graphene Field Effect Transistors: A Route towards Unipolar Characteristics

Paolo Marconcini

Dipartimento di Ingegneria dell'Informazione, Università di Pisa, Via Caruso 16, 56122 Pisa, Italy

Alessandro Cresti

*IMEP-LAHC, UMR 5130 (Grenoble INP/UJF/CNRS/Université de Savoie),
Minatec, 3 Parvis Louis Néel, 38016 Grenoble, France*

François Triozon

CEA LETI-MINATEC, 17 rue des Martyrs, 38054 Grenoble, France

Gianluca Fiori

Dipartimento di Ingegneria dell'Informazione, Università di Pisa, Via Caruso 16, 56122 Pisa, Italy

Blanca Biel

*Dpto. Electrónica y Tecnología de Computadores, Universidad de Granada,
Facultad de Ciencias, Campus de Fuente Nueva, and CITIC,
Campus de Aynadamar, Universidad de Granada E-18071 Granada, Spain*

Yann-Michel Niquet

L_Sim, SP2M, UMR-E CEA/UJF-Grenoble 1, INAC, Grenoble, France

Massimo Macucci

*Dipartimento di Ingegneria dell'Informazione, Università di Pisa, Via Caruso 16, 56122 Pisa, Italy**

Stephan Roche

*CIN2 (ICN-CSIC) and Universitat Autònoma de Barcelona,
Catalan Institute of Nanotechnology, Campus UAB,
08193 Bellaterra (Barcelona), Spain, and ICREA,
Institució Catalana de Recerca i Estudis Avançats, 08070 Barcelona, Spain*

We report fully quantum simulations of realistic models of boron-doped graphene-based field effect transistors, including atomistic details based on DFT calculations. We show that the self-consistent solution of the three-dimensional (3D) Poisson and Schrödinger equations with a representation in terms of a tight-binding Hamiltonian manages to accurately reproduce the DFT results for an isolated boron-doped graphene nanoribbon. Using a 3D Poisson/Schrödinger solver within the Non-Equilibrium Green's Functions (NEGF) formalism, self-consistent calculations of the gate-screened scattering potentials induced by the boron impurities have been performed, allowing the theoretical exploration of the tunability of transistor characteristics. The boron-doped graphene transistors are found to approach unipolar behavior as the boron concentration is increased, and by tuning the density of chemical dopants the electron-hole transport asymmetry can be finely adjusted. Correspondingly, the onset of a mobility gap in the device is observed. Although the computed asymmetries are not sufficient to warrant proper device operation, our results represent an initial step in the direction of improved transfer characteristics and, in particular, the developed simulation strategy is a powerful new tool for modeling doped graphene nanostructures.

The discovery of graphene has opened a promising alternative to silicon-based electronics.¹⁻³ Reported charge mobilities in undoped graphene layers are actually orders of magnitude larger than those measured in silicon, but the unfortunate zero-gap semiconductor nature of this material severely limits the achievable $I_{\text{on}}/I_{\text{off}}$ ratio⁴ (ratio —infinite for an ideal switch— of the current flowing through the device in the conducting state to that flowing in the nonconducting state) for graphene transistors, making them not yet able to compete with mainstream silicon technologies.⁵ Another adverse feature of

graphene-based devices is their ambipolar electrical behavior, which precludes the development of a complementary logic architecture.

A way to induce an energy gap in graphene is to reduce its lateral dimension.⁶⁻⁹ By using e-beam lithographic techniques and oxygen plasma etching processes, graphene nanoribbons (GNRs) down to a width of 10 nanometers can be successfully fabricated.^{10,11} The resulting energy gap, however, is not sufficient for the achievement of a practically useful $I_{\text{on}}/I_{\text{off}}$ ratio in a transistor structure. Chemical, in-solution techniques

have been developed that allow one to obtain nanoribbons with a smaller width^{12,13} but are hard to integrate into a large-scale device production technology. A mixed approach has been followed by Wang and Dai,¹⁴ who use lithography to define the nanoribbons, whose width is then shrunk by means of gas-phase chemical etching. Although quite interesting, this procedure could have some limitation in terms of the achievable device density. Furthermore, energy bandgaps are very unstable with regards to edge reconstruction and defects,¹⁵ thus preventing the fabrication of graphene transistors with performances comparable with their silicon counterparts. Indeed, almost ideal graphene nanoribbons have been obtained by means of careful chemical synthesis,¹⁶ however such an approach cannot be applied to the fabrication of complex circuits on insulating substrates in a straightforward way. Strong chemical damage of graphene could in principle be used to tune the current flow, but with the drawback of a significant decay of the conductance that leads to poor performance in terms of current drive.^{17–21}

Some of us have recently proposed a new class of devices based on the chemical doping of graphene by boron or nitrogen.^{22–24} Using first-principles and mesoscopic quantum transport calculations (within the Landauer-Büttiker formalism) some indications of different behaviors for electrons and holes were predicted in ribbons with lateral sizes as large as 10 nm, with mobility gaps in the order of 1 eV.^{22,23} Here the mobility gaps are typically defined by the corresponding energy window for which the conductance is smaller than a typical value of $G = 10^{-2}G_0$ ($G_0 = 2e^2/h$) (see Ref.²⁵ for details). Recent experimental findings confirmed the possibility to include boron and nitrogen impurities in graphene,^{26–28} therefore suggesting doped graphene transistors as a genuine alternative to ultranarrow GNRs with a more controlled tuning of the conductance features. However, fully self-consistent simulations of doped graphene transistors are mandatory to ascertain the real impact of graphene doping.

We explore the effect, at room temperature, of boron doping in graphene-based field effect transistors using the device geometry illustrated in Fig. 1. Self-consistent NEGF calculations are performed, allowing for a proper treatment of the screened impurity potential and a more robust assessment of the doping effects on the electron-hole transport asymmetry and on the onset of mobility gaps.

I. RESULTS AND DISCUSSION

Parameters for our calculations have been obtained from a first-principle approach, as we detail in the following.

As an initial step, first-principle density functional theory (DFT) calculations were undertaken for a single substitutional boron impurity in two-dimensional (2D) graphene and in GNRs,^{22,23} by means of the SIESTA

code,²⁹ within the local density approximation and using a double- ζ basis set. Following the methodology in Refs.^{23,30}, the onsite energies of the p_z orbitals for the (bulk) 2D case were extracted. Their variation with the distance from the boron atom is shown in Fig. 2 (inset). The boron atom acts as an electron acceptor: the resulting impurity potential is repulsive for electrons and the screening length is found to be of the order of a few angstroms (the screening length³¹ is defined as the distance from the charged impurity at which the surrounding mobile charges, rearranging under the electrostatic action of the impurity, reduce its potential by a factor equal to Euler’s number e).

The transport properties of “quasi-metallic” and semi-conducting armchair GNRs (following Ref.³², we refer to an armchair GNR with N dimers contained in its unit cell as an “N-aGNR”) with a single boron impurity at different sites across the ribbon width are then computed, using the full *ab initio* Hamiltonian, in the Landauer-Büttiker framework.²² Boron impurities actually induce a strong hole backscattering, with much weaker effect on the electron side. A similar result was already obtained in boron-doped carbon nanotubes,^{33,34} and attributed to strong backscattering at the resonance energies of the quasibound states localized around the boron impurity. Due to the lack of the rotational symmetry present in carbon nanotubes, in GNRs the energy of the conductance dip on the hole side depends on the position of the impurity with respect to the ribbon edge (as illustrated in Fig. 2 and Fig. 3).

In Ref.²³ it has been shown that these *ab initio* results can be fairly well reproduced with a simpler tight-binding model with a single orbital per carbon and boron atom. For each atom, the onsite energy is taken as the impurity potential extracted from the *ab initio* calculation. The onsite energy of the boron atom is the only parameter that has to be adjusted in order to achieve the best match between tight-binding and *ab initio* transmission profiles. The success of such a simple tight-binding model in describing boron impurities originates from the preservation of the sp^2 hybridization of graphene in the presence of substitutional boron.

By using this tight-binding model, transport studies in large armchair GNRs with a random distribution of boron atoms, with concentrations between 0.02% and 0.2%, have been performed in Ref.²³. The addition of the transmission dips induced by all impurities leads to a *mobility gap* in the valence band, *i.e.* an energy interval where conductance is nearly suppressed by scattering, while transport in the conduction band is preserved (the opposite behavior would be found in the case of nitrogen doping). This occurs for semiconducting as well as for “quasi-metallic” GNRs, independently of ribbon width, as long as the potential can be assumed to be constant along the channel. The mobility gap increases with boron concentration and ribbon length. Ref.²³ suggested a possible exploitation of this phenomenon to obtain field-effect transistors (FET) with wide GNRs (> 10

nm), within the reach of conventional lithography. The absence of a significant bandgap in these ribbons could be compensated for by the mobility gap. However, the above mentioned study has been performed for ribbons without any gate-induced charge in the channel, since the impurity potential considered was the one extracted directly from an *ab initio* calculation without taking into account the effects of screening when a gate is applied.

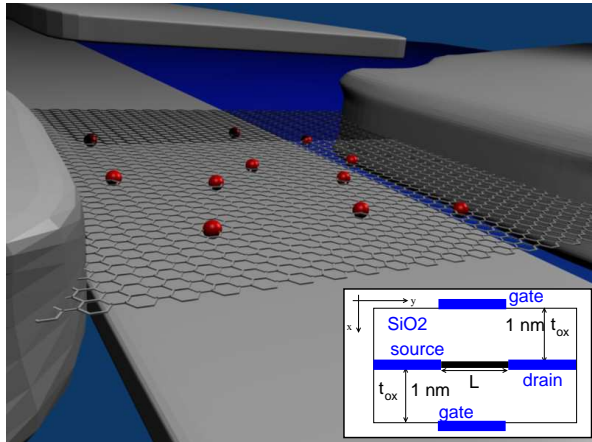


FIG. 1. Sketch of the simulated double gate GNR field effect transistor (FET): red dots represent the substitutional boron atoms. In the inset, the longitudinal cross-section of the transistor is shown (the scale is different along the x and y directions, to make the drawing clearer).

In order to simulate the behavior of a realistic transistor structure, we need to perform a self-consistent calculation to include the effects of an applied gate voltage and of a non-zero drain-source bias on the charge density. This can be done, at a reasonable level of computational complexity, with a tight-binding model set up with parameters properly extracted from the *ab initio* results. However, differently from Ref.²³, the impurity potential obtained from *ab initio* approaches cannot be directly used in a self-consistent simulation, since it would be overscreened, as a result of the Poisson/Schrödinger iterations. The approach chosen here is to mimic DFT self-consistency with the tight-binding model and a proper distribution of fixed charges; then the final impurity potential arises from the tight-binding Poisson/Schrödinger self-consistency.

In particular, as we will detail in the Methods section, the *ab initio* results can be reproduced considering a fixed charge $+e$ (where e is the elementary charge) in correspondence of each carbon atom, and using the following tight-binding representation: null onsite energies are considered in correspondence of all atoms, while, following Ref.³², the hopping parameter is equal to $t_p = -2.7$ eV for all the pairs of nearest neighbor atoms, with the exception of the edge dimers, for which a value of $1.12 t_p$ is used instead.

To validate this approach, a self-consistent Poisson/Schrödinger calculation (described in the Methods

section) is performed for an isolated graphene layer with a single impurity, as in the *ab initio* calculation. As shown in Fig. 2 (inset), the obtained self-consistent potential around the impurity is very close to the *ab initio* result. Also the *ab initio* transmission spectra are accurately reproduced for all positions of the impurity, keeping the boron onsite energy equal to zero and with no further parameter adjustment. Transmission spectra comparisons are shown in Fig. 2.

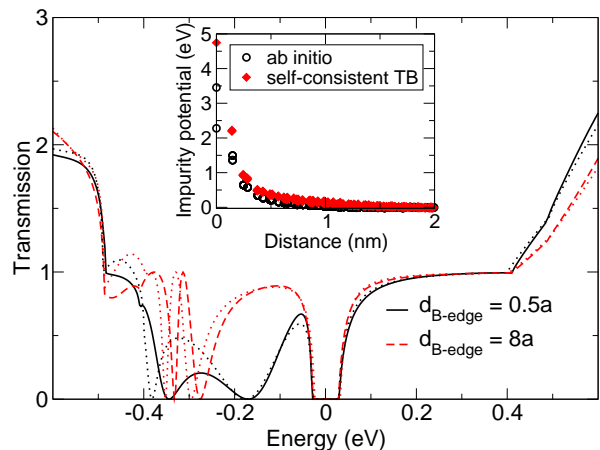


FIG. 2. Transmission through an isolated 32-aGNR (3.81 nm wide) with one boron impurity placed at two different distances from the ribbon edge: $0.5a$ and $8a$, where $a = 2.46$ Å is the hexagonal lattice constant. The bold lines represent the results with our self-consistent tight-binding model. The thin dotted line represents the *ab initio* results. Inset: comparison between the results for the impurity potential in 2D graphene obtained with self-consistent tight-binding and *ab initio* approaches.

Before performing full NEGF calculations, the effect of a gate with a nonzero applied voltage was analyzed on short ribbons with a single impurity. The ribbon is surrounded by a double gate with a dielectric thickness of 1 nm, as shown in Fig. 1. The source-drain voltage and the Fermi level are set to 0. The charge and potential on the ribbon adjust self-consistently as a function of the gate potential V_G . First, the calculation was performed at $V_G = 0$ with vacuum chosen as gate dielectric. The obtained potential is very close to the result discussed above for the neutral isolated ribbon. This gate configuration does not induce any significant additional screening. A more realistic model is obtained by considering a silicon dioxide dielectric between the gate plates and the ribbon, with relative dielectric permittivity $\epsilon_r = 3.9$. However, thin vacuum layers are kept just below and above the ribbon, with a thickness of 0.3 nm, of the order of the calculated graphene/SiO₂ distance.³⁵ The impurity potentials and the corresponding transmission spectra are shown in Fig. 3, for $V_G = 0$ and $V_G = -0.5$ V. Screening is enhanced at a negative gate voltage, due to the

accumulation of holes in the ribbon. This has a strong effect on transmission: the conductance dip is less pronounced and is shifted in energy, which could compromise the presence of a clear mobility gap in a transistor configuration. It was verified that the effect of the gates is much larger than that of the thin air layers, in terms of the global electrostatics, and, in particular, of the screening. This is the reason why in the runs for the evaluation of the transistor characteristics we will not introduce the air layers, that would make convergence of the Poisson-Schrödinger iterations much slower.

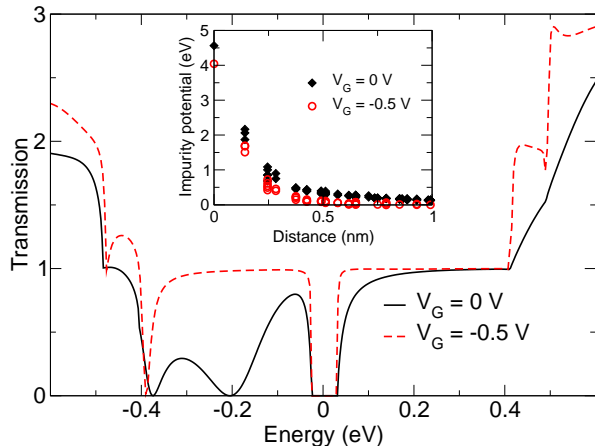


FIG. 3. Influence of the gate voltage on the transmission spectrum of a 32-aGNR with one boron impurity placed at a distance $0.5a$ from the edge. The calculation was performed with silicon dioxide as gate dielectric and a thin vacuum layer surrounding the graphene sheet. Inset: influence of the gate voltage on the impurity potential.

To assess the performance of complete boron-doped graphene transistors biased in a typical operating point, we have used the open-source code NanoTCAD ViDES.³⁶ In this code, the 3D Poisson equation is solved self-consistently with the Schrödinger equation (with open-boundary conditions), within the Non-Equilibrium Green’s Function (NEGF) formalism.³⁷ Schottky contacts have been modeled at the GNR ends with the phenomenological approach described in Ref.³⁸, including self-energies that mimic metallic contacts.

The considered device structure is reported in the inset of Fig. 1. The device is a double-gate FET and the channel is a 32-aGNR (3.81 nm wide) embedded in SiO_2 dielectric. This is consistent with typical nanofabrication techniques, in which the dielectric is deposited after the creation of the drain and source contacts. Top and bottom field oxides are 1 nm thick, and the channel length is equal to 20 nm. In Fig. 4, we show the transfer characteristics of the GNR-FET for a drain-source voltage $V_{DS} = 0.1$ V, for different boron doping concentrations (defined as the ratio of the number of boron atoms to the total number of atoms in the channel). Dopant atoms

are randomly placed along the channel. Results in Fig. 4 refer to a single distribution of dopants.

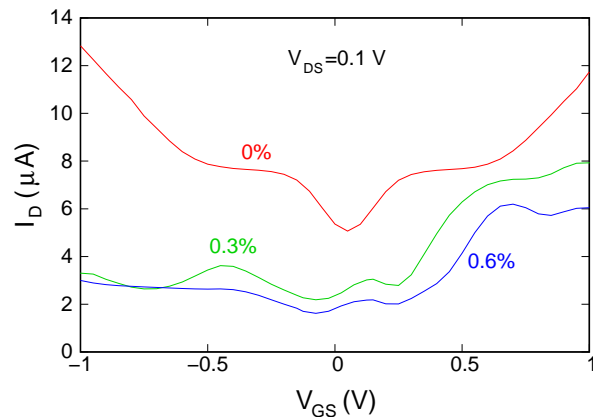


FIG. 4. Transfer characteristics for two different boron doping concentrations (0.3% and 0.6%), for a given random distribution of the dopant atoms. The transfer characteristic for the undoped device is also reported.

As expected, transfer characteristics for the undoped device are symmetric with respect to $V_{GS} = V_{DS}/2 = 0.05$ V. As soon as some boron doping is considered, the p-branch of the $I_{DS}-V_{GS}$ curve is suppressed, as previously observed also in carbon nanotubes.^{33,34} The p-branch suppression increases as the doping concentration is increased. From these results, it appears that with the considered boron doping concentrations, while still not obtaining a sufficient I_{on}/I_{off} ratio for logic applications⁴ with the considered 32-aGNR (which, however, having a “quasi-metallic” behavior in the absence of doping, represents, in this regard, a worst-case scenario), a clear onset of unipolarity occurs. Increasing boron doping, while further reducing the current in the p-branch (due to holes), also leads to a degradation of the device performance above threshold.

In Fig. 5(a)-(b), we show the transfer characteristics for 23 different distributions of doping atoms along the channel, for the same doping concentrations as in Fig. 4. The thick solid lines correspond to the average transfer characteristics computed over the considered statistics of the doping distribution. As can be seen, different doping distributions lead to a large dispersion of the transfer characteristics, which could be reduced if several nanoribbon devices were operated in parallel (as can be necessary in some cases in order to increase the on current).

Nevertheless, we remark that the electron-hole asymmetry is clearly developing with chemical doping, and, based on the results of Ref.²³, it can be strengthened by increasing the gate length up to few hundreds of nanometers (especially for the case with 0.3%). Indeed, longer channel lengths could result in cumulated contributions of multiple scattering effects and localization, which will even more inhomogeneously impact on transport characteristics (as shown in equilibrium situations²³). Due

to computational limitations, we are not reaching such channel lengths here. Computational hurdles, in terms of difficulties in achieving self-consistence, also limit the doping level that can currently be simulated with our method to about 0.6%. Thus, at present we cannot handle the extremely high doping concentrations, of the order of 10%, that have been reached in a recent experiment³⁹ reporting unexpectedly large gap opening effects.

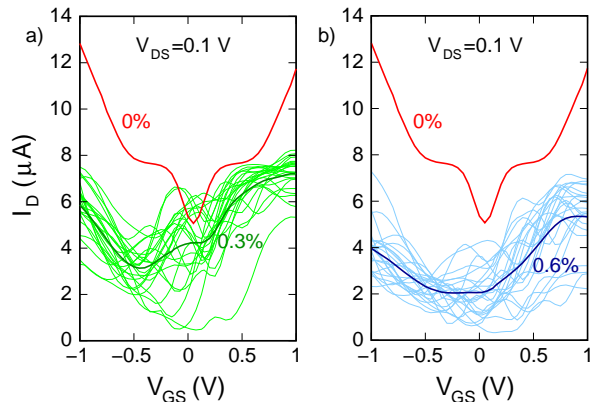


FIG. 5. Transfer characteristics for a) 0.3% and b) 0.6% boron doping concentration, considering a statistics of 23 randomly distributed dopant atoms. The thick solid lines correspond to the average transfer characteristic. For comparison, we report also the transfer characteristic for the undoped device.

II. CONCLUSION

In conclusion, by coupling a DFT-based tight-binding parameterization (validated *via* a multi-scale approach based on *ab initio* techniques) with self-consistent NEGF quantum-mechanical transport simulations, we have found the onset of an electron/hole transport asymmetry and mobility gaps in boron-doped graphene nanoribbon transistors, confirming that chemical doping could serve as a way to shape the current-voltage characteristics of such devices. This is just a first step, because the achieved I_{on}/I_{off} ratio, although for a worst-case condition, is still far too small for practical applications. There is however ample room for improvement and several different approaches could be used to selectively incorporate chemical entities into graphene, thus engineering separate chemically modified areas from a single graphene layer. A doping strategy could therefore be elaborated to implement pn junctions, logic gates and complex architectures directly patterned on the same underlying graphene layer. Conventional state-of-the-art patterning methods, such as e-beam lithography, could be exploited to design superimposed material architectures (with either metallic or other semiconducting materials) onto the selectively doped and functionalized graphene-based substrates. Although our transistor simulations have been

performed for graphene nanoribbons with a width below 5 nm (due to the otherwise prohibitive computational cost), we wish to point out that the scaling analysis detailed in Refs.^{22,23} suggests that our main finding (electron-hole transport asymmetry) should be confirmed for ribbon widths above 10 nm, that is within the reach of conventional fabrication lithography techniques. Finally, longer ribbon lengths and low temperature are also factors which are capable of widening the mobility gaps.²³

III. METHODS

The simulation approach is based on the observation that the DFT results can be recovered performing a self-consistent Poisson/Schrödinger calculation, within the NEGF formalism, on the system, which is described using a tight-binding model and a proper distribution of fixed charges.

In detail, we found that, following this procedure, the tuning of a single parameter of the tight-binding model is sufficient to properly reproduce the *ab initio* impurity potential and transmission spectra. The method is inspired by what actually occurs in the DFT calculation. The total charge of a carbon nucleus and of its core electrons is $+4e$, while it is $+3e$ for boron. In the isolated atoms, this charge is compensated by 4 valence electrons for carbon and 3 valence electrons for boron. In graphene, 3 electrons per atom (including, in the case of doped graphene, the boron atoms) tend to hybridize in a “ sp^2 ” fashion, while the remaining valence electron on each carbon lies on the “ π ” bonding subband formed by the p_z orbitals. Also the p_z orbital on the boron atom is not empty, since it tends to attract an electron from the neighboring carbon atoms, and this determines the shape of the impurity potential shown in Fig. 2. In the single p_z orbital tight-binding approach, the “ sp^2 ” valence electrons are included in the global ionic charge of the atoms, which becomes $+e$ for carbon and 0 for boron. Therefore this is the net charge “localized” on each atom that we have to sum to the negative charge of the p_z atomic orbitals considered in the simulation. As far as the tight-binding parameters are concerned, the onsite energy for carbon atoms is 0, while the hopping energy between nearest neighbors is set to $t_p = -2.7$ eV. The hopping energy of edge dimers is adjusted to $1.12t_p$ in order to reproduce the small bandgap obtained in DFT for “quasi-metallic” N-aGNRs ($N = 3p + 2$, where p is an integer).^{32,40}

Only the onsite energy of boron may be further adjusted, performing a self-consistent Poisson/Schrödinger calculation for an isolated graphene ribbon with a single boron atom and comparing the obtained results with those deriving from the *ab initio* simulation of the same structure.

For the Poisson equation the same boundary conditions are used in the *ab initio* and in the tight-binding calculations: Neumann boundary conditions (*i.e.* derivative of the potential energy, and thus electric field, constant

and, in particular, zero) in the longitudinal direction, at the ends of the nanoribbon, and periodic in the transverse direction, with a separation of 2 nm between the adjacent edges of nanoribbon replicas (indeed, with a large enough separation between the replicas this is equivalent to a Neumann boundary condition). The gate stack has been treated considering a constant permittivity, the one of silicon oxide, between the nanoribbon and each gate, where a Dirichlet boundary condition is assumed. At each iteration, the eigenvalues of the Hamiltonian are computed and the Fermi level is adjusted to obtain charge neutrality. The local charge density is then calculated and the Poisson equation is solved. The obtained electrostatic potential is subtracted from the onsite energies and the process is repeated until self-consistency is achieved. For all of the meshes tested in this work, it was possible to fit the *ab initio* data simply by adjusting the boron onsite energy. A typical choice was to spread the charge of each atom in a spatial region of half-width a_{CC} , the interatomic distance, and to choose a mesh interval of 0.1 nm, small enough to achieve convergence of the Poisson solution. This charge repartition around each atom was defined using a smooth envelope function. In this case, the best fitting was obtained for a value of the boron on-

site energy of about zero, thus substantially coincident with that for carbon.

ACKNOWLEDGMENTS

B.B. acknowledges financial support from the Juan de la Cierva Program and the FIS2008-05805 Contract of the Spanish MICINN. A.C. acknowledges the Fondation Nanosciences *via* the RTRA Dispograph project. We acknowledge the use of the software VMD⁴¹ for graphical design. This work was partly funded by the European Union under Contract No. 215752 GRAND (GRAPhene-based Nanoelectronic Devices), by the French National Research Agency (ANR), in the framework of its 2009 program in Nanosciences, Nanotechnologies & Nanosystems (P3N2009), through the NANOSIM-GRAPHENE project n° ANR-09-NANO-016-01, and by the Italian Ministry for the University and Research (MIUR) through the GRANFET project (n. 2008S2CLJ9). Part of the calculations were performed with the support of the GENCI (Grand Equipment National de Calcul Intensif) initiative.

-
- * m.macucci@mercurio.iet.unipi.it
- ¹ Geim, A. K.; Novoselov, K. S. The Rise of Graphene. *Nat. Mater.* **2007**, *6*, 183–191.
 - ² Novoselov, K. S. Nobel Lecture: Graphene: Materials in the Flatland. *Rev. Mod. Phys.* **2011**, *83*, 837–849.
 - ³ Schwierz, F. Graphene Transistors. *Nat. Nanotechnol.* **2010**, *5*, 487–496.
 - ⁴ ITRS roadmap 2009: <http://www.itrs.net> (accessed May 28, 2012).
 - ⁵ Iannaccone, G.; Fiori G.; Macucci M.; Michetti P.; Cheli M.; Betti A.; Marconcini P. Perspectives of Graphene Nanoelectronics: Probing Technological Options with Modeling. In *Proceedings of IEDM 2009*, Baltimore, USA, December 7-9, 2009; IEEE Conference Proceedings: 2009; pp. 245–248.
 - ⁶ Nakada, K.; Fujita, M.; Dresselhaus, G.; Dresselhaus, M. S. Edge State in Graphene Ribbons: Nanometer Size Effect and Edge Shape Dependence. *Phys. Rev. B* **1996**, *54*, 17954–17961.
 - ⁷ Brey, L.; Fertig, H. A. Electronic States of Graphene Nanoribbons Studied with the Dirac Equation. *Phys. Rev. B* **2006**, *73*, 235411.
 - ⁸ Castro Neto, A. H.; Guinea, F.; Peres, N. M. R.; Novoselov, K. S.; Geim, A. K. The Electronic Properties of Graphene. *Rev. Mod. Phys.* **2009**, *81*, 109–162.
 - ⁹ Marconcini, P.; Macucci, M. The $k \cdot p$ Method and Its Application to Graphene, Carbon Nanotubes and Graphene Nanoribbons: the Dirac Equation. *Riv. Nuovo Cimento Soc. Ital. Fis.* **2011**, *34*, 489–584. See also <http://brahms.iet.unipi.it/supplem/reviewgraph.html> (accessed May 28, 2012).
 - ¹⁰ Han, M. Y.; Özyilmaz, B.; Zhang, Y.; Kim, Ph. Energy Band-Gap Engineering of Graphene Nanoribbons. *Phys. Rev. Lett.* **2007**, *98*, 206805.
 - ¹¹ Han, M. Y.; Brant, J. C.; Kim, Ph. Electron Transport in Disordered Graphene Nanoribbons. *Phys. Rev. Lett.* **2010**, *104*, 056801.
 - ¹² Wang, X.; Ouyang, Y.; Li, X.; Wang, H.; Guo, J.; Dai, H. Room-Temperature All-Semiconducting Sub-10-nm Graphene Nanoribbon Field-Effect Transistors. *Phys. Rev. Lett.* **2008**, *100*, 206803.
 - ¹³ Li, X.; Wang, X.; Zhang, L.; Lee, S.; Dai, H. Chemically Derived, Ultrasoft Graphene Nanoribbon Semiconductors. *Science* **2008**, *319*, 1229–1232.
 - ¹⁴ Wang, X.; Dai, H. Etching and Narrowing of Graphene from the Edges. *Nature Chem.* **2010**, *2*, 661–665.
 - ¹⁵ Cresti, A.; Nemeč, N.; Biel, B.; Niebler, G.; Triozon, F.; Cuniberti, G.; Roche, S. Charge Transport in Disordered Graphene-Based Low Dimensional Materials. *Nano Res.* **2008**, *1*, 361–394.
 - ¹⁶ Cai, J.; Ruffieux, P.; Jaafar, R.; Bieri, M.; Braun, T.; Blankenburg, S.; Muoth, M.; Seitsonen, A. P.; Saleh, M.; Feng, X.; *et al.* Atomically Precise Bottom-Up Fabrication of Graphene Nanoribbons. *Nature* **2010**, *466*, 470–473.
 - ¹⁷ Moser, J.; Tao, H.; Roche, S.; Alzina, F.; Sotomayor Torres, C. M.; Bachtold, A. Magnetotransport in Disordered Graphene Exposed to Ozone: From Weak to Strong Localization. *Phys. Rev. B* **2010**, *81*, 205445.
 - ¹⁸ Leconte, N.; Moser, J.; Ordejón, P.; Tao, H.; Lherbier, A.; Bachtold, A.; Alsina, F.; Sotomayor Torres, C. M.; Charlier, J. C.; Roche, S. Damaging Graphene with Ozone Treatment: A Chemically Tunable Metal-Insulator Transition. *ACS Nano* **2010**, *4*, 4033–4038.
 - ¹⁹ Leconte, N.; Lherbier, A.; Varchon, F.; Ordejon, P.; Roche, S.; Charlier, J.-C. Quantum Transport in Chemically Modified Two-Dimensional Graphene: From Mini-

- mal Conductivity to Anderson Localization. *Phys. Rev. B* **2011**, *84*, 235420.
- ²⁰ Cresti, A.; Lopez-Bezanilla, A.; Ordejón, P.; Roche, S. Oxygen Surface Functionalization of Graphene Nanoribbons for Transport Gap Engineering. *ACS Nano* **2011**, *5*, 9271–9277.
- ²¹ Bruzzone S.; Fiori G. *Ab-Initio* Simulations of Deformation Potentials and Electron Mobility in Chemically Modified Graphene and Two-Dimensional Hexagonal Boron-Nitride. *Appl. Phys. Lett.* **2011**, *99*, 222108.
- ²² Biel, B.; Blase, X.; Triozon, F.; Roche, S. Anomalous Doping Effects on Charge Transport in Graphene Nanoribbons. *Phys. Rev. Lett.* **2009**, *102*, 096803.
- ²³ Biel, B.; Triozon, F.; Blase, X.; Roche, S. Chemically Induced Mobility Gaps in Graphene Nanoribbons: A Route for Upscaling Device Performances. *Nano Lett.* **2009**, *9*, 2725–2729.
- ²⁴ Lherbier, A.; Biel, B.; Niqet, Y.-M.; Roche, S. Transport Length Scales in Disordered Graphene-Based Materials: Strong Localization Regimes and Dimensionality Effects. *Phys. Rev. Lett.* **2008**, *100*, 036803.
- ²⁵ Cresti, A.; Roche, S. Range and Correlation Effects in Edge Disordered Graphene Nanoribbons. *New J. Phys.* **2009**, *11*, 095004.
- ²⁶ Zhao, L.; He, R.; Rim, K. T.; Schiros, T.; Kim, K. S.; Zhou, H.; Gutiérrez, C.; Chockalingam, S. P.; Arguello, C. J.; Pálová, L.; *et al.* Visualizing Individual Nitrogen Dopants in Monolayer Graphene. *Science* **2011**, *333*, 999–1003.
- ²⁷ Usachov, D.; Vilkov, O.; Grüneis, A.; Haberer, D.; Fedorov, A.; Adamchuk, V. K.; Preobrajenski, A. B.; Dudin, P.; Barinov, A.; Oehzelt, M.; *et al.* Nitrogen-Doped Graphene: Efficient Growth, Structure, and Electronic Properties. *Nano Lett.* **2011**, *11*, 5401–5407.
- ²⁸ Lin, T.; Huang, F.; Liang, J.; Wang, Y. A Facile Preparation Route for Boron-Doped Graphene, and its CdTe Solar Cell Application. *Energy Environ. Sci.* **2011**, *4*, 862–865.
- ²⁹ Soler, J. M.; Artacho, E.; Gale, J. D.; García, A.; Junquera, J.; Ordejón, P.; Sánchez-Portal, D. The SIESTA Method for *Ab Initio* Order-*N* Materials Simulation. *J. Phys.: Condens. Matter* **2002**, *14*, 2745–2779.
- ³⁰ Adessi, Ch.; Roche, S.; Blase, X. Reduced Backscattering in Potassium-Doped Nanotubes: *Ab Initio* and Semiempirical Simulations. *Phys. Rev. B* **2006**, *73*, 125414.
- ³¹ Stern, F. Elementary Theory of the Optical Properties of Solids. In *Solid State Physics. Advances in Research and Applications*; Seitz F., Turnbull D., Eds.; Academic Press: New York, 1963; Vol. 15, pp 299–408.
- ³² Son, Y.-W.; Cohen, M. L.; Louie, S. G. Energy Gaps in Graphene Nanoribbons. *Phys. Rev. Lett.* **2006**, *97*, 216803.
- ³³ Choi, H. J.; Ihm, J.; Louie, S. G.; Cohen, M. L. Defects, Quasibound States, and Quantum Conductance in Metallic Carbon Nanotubes. *Phys. Rev. Lett.* **2000**, *84*, 2917–2920.
- ³⁴ Avriller, R.; Roche, S.; Triozon, F.; Blase, X.; Latil, S. Low-Dimensional Quantum Transport Properties of Chemically-Disordered Carbon Nanotubes: from Weak to Strong Localization Regimes. *Mod. Phys. Lett. B* **2007**, *21*, 1955–1982.
- ³⁵ Hossain, M. Z. Chemistry at the Graphene-SiO₂ Interface. *Appl. Phys. Lett.* **2009**, *95*, 143125.
- ³⁶ Fiori, G.; Iannaccone, G. Simulation of Graphene Nanoribbon Field-Effect Transistors. *IEEE Electron Device Lett.* **2007**, *28*, 760–762. Code is available at “NanoTCAD ViDES,” DOI: 10254/nanohub-r5116.5. <http://nanohub.org/resources/vides/> (accessed May 28, 2012).
- ³⁷ Datta, S. *Quantum transport: Atom to transistor*; Cambridge University Press: Cambridge, United Kingdom, 2005.
- ³⁸ Guo, J.; Datta, S.; Lundstrom, M.; Anantram, M. P. Towards Multiscale Modeling of Carbon Nanotube Transistors. *Int. J. Multiscale Comput. Eng.* **2004**, *2*, 257–276.
- ³⁹ Tang, Y.-B.; Yin, L.-C.; Yang, Y.; Bo, X.-H.; Cao, Y.-L.; Wang, H.-E.; Zhang, W.-J.; Bello, I.; Lee, S.-T.; Cheng, H.-M.; *et al.* Tunable Band Gaps and p-Type Transport Properties of Boron-Doped Graphenes by Controllable Ion Doping Using Reactive Microwave Plasma. *ACS Nano* **2012**, *6*, 1970–1978.
- ⁴⁰ Fujita, M.; Igami, M.; Nakada, K. Lattice Distortion in Nanographite Ribbons. *J. Phys. Soc. Jpn.* **1997**, *66*, 1864–1867.
- ⁴¹ Humphrey, W.; Dalke, A.; Schulten, K. VMD: Visual Molecular Dynamics. *J. Molec. Graphics* **1996**, *14*, 33–38. See <http://www.ks.uiuc.edu/Research/vmd/> (accessed May 28, 2012).